The influence of drug solubility and sampling frequency on metformin and glibenclamide release from double-layered particles: experimental analysis and mathematical modelling

Journal:	*Journal of the Royal Society Interface*
Manuscript ID	rsif-2019-0237.R1
Article Type:	Research
Date Submitted by the Author:	17-May-2019
Complete List of Authors:	Shams, Talayeh; University College London, Department of Mechanical Engineering; University College London, School of Pharmacy Brako, Francis; University College London School of Pharmacy; University College London Department of Mechanical Engineering Huo, Saguo; London Centre for Nanotechnology Harker, Anthony; University College London, Department of Physics and Astronomy and London Centre for Nanotechnology Edirisinghe, Mohan; University College London, Department of Mechanical Edirisinghe, Ursula; Hillingdon Hospital, Accident and Emergency Department
Categories:	Life Sciences - Engineering interface
Subject:	Biomaterials < CROSS-DISCIPLINARY SCIENCES
Keywords:	electrospraying, diabetes mellitus, metformin, glibenclamide, depot formulations

SCHOLARONE™
Manuscripts

The influence of drug solubility and sampling frequency on metformin and glibenclamide release from double-layered particles: experimental analysis and mathematical modelling

T. Shams[1, 2], F. Brako[1, 2], S. Huo[3], A. H. Harker[4], U. Edirisinghe[5], M. Edirisinghe[1*]

[1]Department of Mechanical Engineering, University College London, Torrington Place, London, WC1E 7JE, UK

[2]Department of Pharmaceutics, University College London School of Pharmacy, Brunswick Square, London, WC1N 1AX, UK

[3]London Centre for Nanotechnology, Kings Cross, London, WC1H 0AH, UK

[4]Department of Physics and Astronomy and London Centre for Nanotechnology, University College London, London, WC1E 6BT, UK

[5]Accident and Emergency Department, Chelsea and Westminster Hospital, London SW10 9NH, UK

Corresponding author: m.edirisinghe@ucl.ac.uk

Keywords: Electrospraying; depot formulations; diabetes mellitus; metformin; glibenclamide

Abstract

Co-axial electrohydrodynamic atomization was used to prepare core/shell polymethylsilsesquioxane particles for co-delivery of metformin and glibenclamide in a sustained release manner. The drug-loaded microparticles were mostly spherical and uniformly distributed in size, with average diameters between 3 and 5µm across various batches. FTIR was used to confirm the presence of drugs within the particles while X-ray diffraction studies revealed drugs encapsulated existed predominantly in the amorphous state. Intended as systems that potentially can act as depot formulations for long term release of antidiabetics, a detailed analysis of drug release from these particles was necessary. Drugs of different solubilities were selected in order to study the effects of drug solubility from a core/shell particle system. Further analyses to determine how conditions such as release into a limited volume of media, sampling rate and partitioning of drug between the core and shell layers influenced drug release were conducted by comparing experimental and mathematically modelled outcomes. It was found that while solubility of drug may affect release from such systems, rate of removal of drug (sampling frequency) which upsets local equilibrium at the particle/solution interface prompting a rapid release to redress the equilibrium influenced release more.

1. Introduction

The International Diabetes Federation estimated about 415 million adults as having diabetes as at 2015 and projected this figure to be 642 million by 2040. About 90% of these are classified under Type2 diabetes, a condition mainly driven by obesity, sedentary lifestyle and increased consumption of unhealthy diets including sugar-sweetened beverages [1, 2]. Oral administration of hypoglycaemic agents, often a biguanide, e.g. metformin, has predominantly been the first line option when medication is required for managing type 2 diabetes mellitus [3, 4]. Defective insulin sensitivity and defective insulin secretion typically coexist in most patients with type 2 diabetes. These two abnormalities contribute to hyperglycaemia [5]. Thus, oral therapy with either biguanides such as metformin that increase sensitivity of peripheral tissues to insulin, or sulfonylureas such as glibenclamide, which stimulate insulin secretion, are sensible approaches to type 2 diabetes mellitus [6]. Considering metformin's utility as an antidiabetic drug as well as some desired physical properties such as aqueous solubility, novel formulations that enable its controlled release for prolonged duration in order to obtain maximum absorption and better bioavailability are highly desirable. For this reason, metformin was selected as a model drug for biguanides. For sulfonylureas, glibenclamide was selected as a model drug due to its poor solubility in water, which in turn causes its limited dissolution and absorption. The low oral bioavailability of the conventional glibenclamide tablets necessitates a formulation approach that could improve upon its poor solubility. These issues have led to large variation in glibenclamide bioavailability between different commercial brands with each brand presenting inter-subject variability.

Sulfonylureas are thought to act by binding to sulfonylurea receptor (SUR)-1 subunits of

pancreatic beta potassium channels leading to their closure and subsequent membrane depolarization which open up voltage-dependent Ca^{2+} channels. This ensures a build-up of intracellular calcium concentrations, consequentially mediating the release of insulin [7]. Biguanides on the other hand work through complex physiological pathways mediated by both AMP-activated protein kinase (AMPK)-dependent and AMPK-independent mechanisms to reduce hepatic glucose production [8].

Each of them can be used solely or in combined form when either of them on their own is not sufficient on bringing down or maintaining blood sugar at safe levels. However, there remain issues of patient non-adherence which are generally driven by multiple daily dosing requirements [9, 10]. Considering how effective these active pharmaceutical ingredients have been in oral formulations for the control of blood sugar levels, the potential of formulating these as depot preparations for long-term release is an appealing proposal. Micro and nanoparticle formulations of these hypoglycaemic agents to be delivered parenterally could offer a more effective control of blood sugar levels as these drug-loaded particles have a number of advantages including versatility with regards to delivery for local or systemic effects as well as ease with which they are injected into tissues or intravenously [11].

In this study, electrohydrodynamic (EHD) forming has been utilized in developing core-shell particle structures [12] where either glibenclamide (model sulfonylurea drug) or metformin (model biguanide drug) occupies the core while polymethylsilsesquioxane (PMSQ) polymer makes the shell surrounding the active ingredient [13, 14] . PMSQ was chosen as it offers chemical durability and being biocompatible, it is a desirable material for applications in biomedical engineering. In addition to its biocompatibility and durability, its high hydrophobicity ensures low moisture uptake; a feature that can

ultimately be valuable for stability of drugs upon storage. Finally, PMSQ is known to have physical characteristics that allow them to be processed into hollow spheres [15, 16]. As this study explored the possibility of formulating core-shell particles which potentially can be administered parenterally for drug release over extended periods, the features offered by PMSQ i.e. stability, compatibility, hydrophobicity and processability underscored the rational for selecting this polymer for our investigations. With respect to drugs, the remarkable water solubility differences between metformin and glibenclamide, in addition to being routinely used oral hypoglycaemic agents, were the reasons for selecting the two [17]. The disparities in water solubility of the two drugs made it possible for the influence of solubility on drug release from these particles to be studied [18, 19]. Various microscopic and spectroscopic techniques were employed in elucidating the physical characteristics and molecular composition of these structures. To determine the possibility of metformin and glibenclamide particles functioning as depot drug releasing systems, a more detailed view of release profiles as influenced by particle composition, morphology and physical properties was developed. Furthermore, the likely effects of varying experimental procedures such as frequency of sampling which hitherto had been considered inconsequential to release outcomes were studied. Trends observed as well as mathematical modelling of experimental data derived from release data are discussed, offering further insights into the release of drug from a system essentially made of uniformly distributed bi-layered spherical particles.

2. Materials and Methods

2.1 Materials

Polymethylsilsesquioxane (PMSQ) with an average molecular weight of 7465 g mol^{-1} was provided by Wacker Chemie AG, GmbH (Burghausen, Germany). Metformin

hydrochloride with molecular weight of 165.62 g mol^{-1} was obtained from Sigma-Aldrich (Poole, UK). Glibenclamide with molecular weight 494.61 g mol^{-1}, used in this work was purchased from MP Biomedicals (Loughborough, UK). Research grade ethanol (99% purity) was purchased from Sigma-Aldrich (Poole, UK). All of the above were used as received.

2.2.1 Preparation of the electrospraying solutions containing polymer and active ingredients.

A 15% (w/v) PMSQ solution was prepared by dissolving an appropriate amount of PMSQ in ethanol and stirred to ensure complete dissolution. To prepare the metformin particles (S1), 10 mg of the drug was dissolved in 80 ml of ethanol, and for glibenclamide particles (S2), 20 mg glibenclamide was dissolved in 80 ml ethanol. For the combined drug formulation (S3), 10 mg metformin and 20 mg glibenclamide were dissolved in 80 ml ethanol. Ethanol was used as both drugs as well as PMSQ are freely soluble in it and rapidly evaporates during electrospraying. Characteristics of the prepared solutions including electrical conductivity, surface tension and viscosity, measured at ambient conditions, are shown in Table 1. Electrical conductivity was determined using a conductivity probe, Jenway 3540 pH/conductivity meter (Cole-Palmer, Stone, UK). Viscosity was measured using a U-tube viscometer 75 mL Cannon- Fenske Routine Viscometer (Cannon Instruments, Pennsylvania, USA), while a Kruss tensiometer Model-K9 (Kruss GmbH, Hamburg, Germany) was used to obtain surface tension values. Distilled water was used to calibrate the viscometer, tensiometer and electrical conductivity probe.

Table 1 Properties of solutions used in developing the particles

Solution	Surface Tension (mN/m)	Viscosity (mPa s)	Electrical Conductivity (µS/m)
Metformin HCL 10mg in 80ml EtOH	21.2 ± 0.3	0.92	25.4 ± 0.3
Glibenclamide 20mg in 80 ml EtOH	21.4 ± 0.2	0.97	32.3 ± 0.3
10mg Metformin HCL + 20mg Glibenclamide in 80ml EtOH	21.5 ± 0.2	0.93	23.2 ± 0.4
PMSQ 15% w/v in EtOH	21.8 ± 0.3	1.36	0.66 ± 0.0

2.2.2   Preparation of the drug delivery systems

The prepared solutions were carefully placed into 10 mL airtight syringes to avoid

bubble formation during processing, and set to be driven by a pump, Harvard PHD

4400 (Harvard Apparatus, Edenbridge, UK) to deliver precise volume per unit time. A

co-axial needle system with inner diameters of 0.6 mm and 1.52 mm and outer

diameters of 0.9 mm and 2.03 mm, were connected to a high precision voltage power

supply. The positive electrode of a high precision DC voltage power supply HCP 35

65000 (Fug Elektronik, Rosenheim, Germany) was connected to the needle tip. The

ground electrode was fixed onto a rectangular metal collector plate. Experiments

were carried out under ambient conditions with average room temperature of 21℃

and relative humidity of 40-60% throughout the studies. Electrical potential was

applied across a fixed working distance of 150 mm between the tip of the co-axial

needles tip and the grounded collection platform. The flow rates and the range of

applied voltages were tuned in order to establish a stable cone-jet for each system.

Different spherical structures incorporating single or two drugs in the core

surrounded by outer polymeric layer were made subsequently. The optimal

combinations of flow rates and applied voltage that enabled the processing of various

batches of particles are shown in Table 2.

Table 2 Experimental parameter for each polymeric system

Polymer System	Inner Flow Rate (μl/min)	Outer Flow Rate (μl/min)	Applied Voltage (kV)
S1: Metformin-loaded particles	2	8	11
S2: Glibenclamide-loaded particles	6	18	12
S3: Metformin + Glibenclamide-loaded particles	6	18	11

2.2.3 Particle morphology and size distribution

Drug-loaded microparticles were examined by scanning electron microscopy (SEM). The

particles were gold sputter-coated with a rotary pump coater Q150R ES (Quorum

Technologies, Laughton, UK) for 3 min preceding SEM imaging by Hitachi S-3400n

(Hitachi High Technologies, Tokyo, Japan). The size distributions of the particles were

obtained from SEM images using Image J software, where the diameter measurements of

300 particles from each batch were taken randomly and the mean diameter was

calculated. The size distribution curves were obtained by examining raw measurements

using the Image J application (National Institutes of Health, Maryland, USA) and OriginPro

software (OriginLab, Northampton, USA). The images and corresponding size

distributions are shown in Figure 1.

2.2.4 *X-ray powder diffraction*

The particle structures and loaded active ingredients were studied using D/Max-BR diffractometer (RigaKu, Tokyo, Japan) with Cu Kα radiation. Analyses were conducted at 40 mV and 30 mA over 2θ range of 5–45° at a rate of 2°/min. Data obtained were converted to diffractograms and evaluated using OriginPro 7.0 software (OriginLab Corporation, Northampton, USA).

2.2.5 *Fourier transform infrared spectroscopy (FTIR)*

In order to establish if the particles produced contained active ingredients as intended, the chemical compositions of the particles were investigated using Attenuated Total Reflection Fourier Transform Infrared spectroscopy (ATR–FTIR) measurements (Bruker Vertex 90 spectrometer), and spectrographs were interpreted using OPUS Viewer version 6.5 software. Each sample had 64 scans at a resolution of 4 cm^{-1}. Spectra of the particles were compared to those of the individual drugs and polymers to identify characteristic functional groups in the processed materials. The same parameters were used for background scans before each sample was analysed.

2.2.6 *Focused ion beam (FIB) microscopy*

Cross sectional images of the particles were prepared using ZEISS NV40 FIB/SEM, a cross-beam of focused ion and field emission gun (FEG) electron beam. In the experiments, an ion beam 30 kV, 150-300 pA is used to cut the sphere sample and 1.5 kV was used for imaging the cross section using BSE detector. Particles were gold sputtered for 120 s and mounted on metallic studs.

2.2.7 Drug release studies

To measure the amount of drug released from drug-loaded microparticles, a setup in which 40mg of sample was enclosed in a fine metal mesh to ensure total immersion of particles and was placed in a vessel of 40 ml capacity. Body temperature conditions and continuous agitation at 80 rpm were maintained throughout the release study using a benchtop incubated shaker (Sciquip, Newtown, UK). Samples volume of 2 ml were taken at various intervals from the vessel. 2 ml blank media was added after each sampling to maintain a constant volume.

Ultraviolet-visible (UV-Vis) spectroscopy (Jenway 6305 UV/Visible spectrophotometer, Bibby Scientific, Staffordshire, UK) operating at 231 nm was used to quantify amount of metformin sampled during this study. The operating wavelength was obtained after a spectrum scan of 0.003 mg/mL standard metformin solution between 200 and 280 nm. To convert absorbance readings to drug concentrations, a calibration curve and equation were obtained by measuring absorbance of standard metformin solutions in concentrations between 0.0008 and 0.003 mg/mL, from which metformin content in microparticles were derived. The same procedure was undertaken for quantification of glibenclamide at detection wavelength of 300 nm.

3 Results and discussions

3.1 Particle size and size distribution

SEM images from the three batches were analysed for size and size distribution. The mean particle size (see Figure 1) was lowest for S2 at 1.66 ± 0.74 μm. This may be attributable to the highest electrical conductivity of the inner solution containing glibenclamide which aids EHD forming. In comparison, for S3, with the same set flow rates, owing to a lower applied voltage and electrical conductivity of the inner solution,

the average particle size is higher at 4.79 ± 0.48 μm. The same reason possibly explains

the differences seen between S1 and S2. When compared, S2 contained an inner solution

with lower electrical conductivity and hence required lower applied electrical potential.

This resulted in a slight increase in the average particle size (3.44 ± 0.44 μm)

Figure 1: SEM images and the corresponding size distribution graphs of the developed drug delivery systems S1, S2 and S3. The smooth curve superimposed on each histogram represents a normal distribution with the same mean and standard deviation as the sample.

The differences in the flow rates of S1 compared to that of S2 and S3 were due to

formation of an unstable cone-jet that resulted in wide distribution size and

inconsistency. Therefore the selected values were chosen to ensure a narrow particle size

distribution, which is of immense importance in development of drug delivery system.

3.2 Structure and composition

The XRD patterns of the unprocessed PMSQ, metformin and glibenclamide as well as

those of the prepared formulations are shown in Figure 2.

Figure 2: XRD spectrum of a) pure metformin HCL, glibenclamide and PMSQ and b) the developed formulations S1, S2 and S3.

The sharp diffraction peaks, representative of pure metformin were notable at 2θ angles

of 17º, 22º, 23º, 25.27º and 45º. This series of sharp and intense diffraction peaks are

indicative of the crystalline state of pure metformin. The diffraction spectrum of pure

glibenclamide also showed high peak intensities in the region of 12º to 34º of 2θ,

indicating its crystalline state [20]. PMSQ showed the characteristic broad humps of an amorphous materials.

As observed in the diffractograms acquired for the developed formulation (S1 – S3), the amorphous nature was most prominent. In all formulations, no characteristic peaks of metformin and glibenclamide were detected. As revealed in the X-ray diffractograms of the drug-loaded formulations, the physical states of these particles are predominantly in amorphous state. The absence of the characteristic sharp peaks seen in the pure drugs indicate an amorphous solid dispersion of the drugs in the polymer, as well as the relatively low amounts of drugs present in the core-shell particles.

3.3 Particle composition

The molecular compositions of the particles and possible interactions between drug and polymer during processing were investigated by FTIR. Spectra of the raw materials and the particles produced are shown in Figure 3. A characteristic band for PMSQ was observed at 1130 cm^{-1} [16]. The spectrum of metformin showed characteristic bands at 3369 cm^{-1} and 3294 cm^{-1}, pointing to a primary amine (N-H) stretching vibration and a band at 3155 cm^{-1} arising from secondary amine stretching. Characteristic bands at 1622 cm^{-1} and 1567 cm^{-1}, assigned to C-N stretching were also observed. The spectrum obtained for glibenclamide showed characteristic amide peaks at 3369 cm^{-1}, 3316 cm^{-1} and 1715 cm^{-1}. The urea carbonyl and N-H stretching vibrations were also observed at 1615 cm^{-1} and 1526 cm^{-1}, respectively. The absorption bands between 2800 cm^{-1} and 3200 cm^{-1} represent the aliphatic and aromatic C-H bond in this drug. The results obtained agreed with the published spectrum for the pure drugs [21].

Figure 3: FTIR spectra of pure PMSQ, metformin HCL, glibenclamide and the developed formulations S1, S2 and S3.

The FTIR spectra obtained for the developed formulations predominantly reflected peaks corresponding to PMSQ. This is to be expected as the formed particles were largely composed of PMSQ. Nonetheless, peaks at 1567 cm^{-1}, 1622 cm^{-1} and 1715 cm^{-1} though significantly diminished to reflect the quantities of drugs entrapped were also present, implying that indeed the particles contained drugs as intended. The absence of any new peaks or insignificant shifts in original peaks, when compared to spectra of either drugs or polymers indicated non-existent intermolecular interactions among the polymers and drugs.

3.4 Particle morphology

The morphology of the prepared formulations was studied using FIB/SEM (Fig. 4). The particles show a well-defined outer shell that encompasses a core, where the majority of the encapsulated drug is resident. The cross-sectional cuts through the particles are indicative of a porous core most likely created by spaces left following evaporating solvents escaping during particle formation. The outermost portion of the particle though appear to be less porous as the polymer solution from which this layer was formed had less amount of evaporating solvent, compared to the drug solution that formed the core (S1, S2 and S3).

Figure 4: SEM/FIB cross-section images of the prepared formulations S1, S2 and S3.

3.5 Drug release

A major part of this paper is dedicated to the release of antidiabetic drugs of different solubilities from polymeric nanoparticles through a combination of experimental data analysis and mathematical modelling.

3.5.1 Influence of particle size and morphology

The release profile of metformin was studied from formulations S1 and S3 for a duration of 12 hours and 168 hours respectively (Figure 5a).

Figure 5: Cumulative drug release in the first 5 hours of a) metformin from S1 and S3 formulations b) glibenclamide from S2 and S3 formulations and c) cumulative release of glibenclamide and metformin percentage cumulative release from S3.

Burst release can be observed for the first 5 hours. This can be explained by diffusion of metformin towards the surface of the polymeric shell as solvent evaporation takes place. The slightly higher dissolution rate of the drug from S3 at 39% can be due to the slightly larger particle size of 4.79 ± 0.48 μm that allows the incorporation of more unit surface bound drug per surface area.

The burst release of metformin from S1 was 26% within the first 5 hours of drug release. Moreover, the flow rate ratio of metformin solution to PMSQ solution is higher for S3 at weight ratio 1:3 when compared to that of S1 at 1:4, this may explain the slight discrepancies of metformin burst release from the formulation containing both metformin and glibenclamide. A similar set of observations were made for glibenclamide (Figure 5b), the initial burst release was slightly higher from S3 when compared to S2. The EHD flow rates ratio was kept the same for both formulations. Therefore, the slightly

higher dissolution rate of glibenclamide from S3 may be explained by more surface bound

drug content in those, considering they are larger than S2. The burst release was also

compared for that of glibenclamide and metformin from S3 to better understand the

effect of aqueous drug solubility. As can be concluded from Figure 5c, metformin

encountered notably higher dissolution rate which may be attributable to higher water

solubility and hence relatively faster diffusion from the polymeric particles to the release

medium. This effect is expected for highly water-soluble drugs. After the first 5 hours of

burst release, metformin and glibenclamide release from the combined S3 formulation

nearly followed the same path (Figure 6a), resembling zeroth order release. Due to the

hydrophobic nature of the PMSQ polymeric carrier, the drug release is mainly driven by

diffusion against the concentration gradient. Thus, movement of drug molecules from the

core, an area with higher drug concentration through channels created within the

particles occurred in order to reach an equilibrium state between the particles and

dissolution media. It is evident from the release profiles, that the frequency of sampling

can also affect the dissolution rate, and this is considered in detail in section 3.5.2 below.

Figure 6 a) Glibenclamide and metformin cumulative release from S3 and b) glibenclamide and metformin cumulative release from S2 and S1.

Higher sampling frequency causes more disturbance to the system and results in further

agitation of the drug delivery systems, which in turn also increases the dissolution rate

as the release medium is continuously refreshed after aliquots are taken. The dissolution

rate increases as there is a shorter time interval in between each sampling. An example

of this can be seen in Figure 6a. For operational reasons samples were taken at 5, 20, 24

and 48 hours, and the effect of the short interval between 20 and 24 hours can be seen as

a steep section of the release fraction. The same effect can be seen in Figure 7a and will be discussed in more detail in section 3.3.5 below.

As shown in Figure 6b, the glibenclamide release from S2 follows zeroth order release after the initial bust release for the first 5 hours, at which point the frequency of sampling was decreased and samples were withdrawn on hourly basis. The same was done for metformin HCL release studies from S1 formulation. Although glibenclamide is a poorly water-soluble drug, the dissolution rate was slightly higher when compared to metformin, which may be due to smaller average particle size of 1.66 ± 0.74 μm. This means that there was a higher surface area to volume ratio which resulted in a higher dissolution rate of the incorporated drug. This feature of microparticles make them highly favourable for encapsulation of drugs with low aqueous solubility as the increased surface area enhance their dissolution. There was little difference between the release of metformin and glibenclamide suggesting that the hydrophilic nature of the incorporated drug had little effect on the dissolution rate. The improved dissolution rates, even among the system with hydrophobic drug agree with previous studies that have reported, that in general, electrospraying results in formation of microparticles that incorporate the active ingredient in their amorphous state, resulting in an accelerated drug release [22]. It should be noted that there was higher initial amount of glibenclamide in the prepared formulations when compared to that of metformin, which to some extent reflects the initial amounts of drugs incorporated in the particles; 10mg of metformin for S1, 20 mg of glibenclamide for S2 and for the combined drug formulation (S3), 10 mg metformin and 20 mg glibenclamide were used.

3.5.2 The effect of drug solubility vs sampling rate on drug release

Theoretical modelling of drug release from particles usually assumes the so-called perfect sink conditions – that is, the concentration of the active ingredient in the medium outside the particles is assumed to be negligible. The importance of maintaining appropriate conditions has been noted in the past [23]. It is relatively straightforward to describe this effect. If fluid were to be kept flowing past the particles, so that the particles were always surrounded by fluid containing no active ingredient, then eventually all of the active ingredient could be dissolved. In general, though, release rates are measured in a fixed volume of fluid, so the active ingredient may build up to a significant concentration. Suppose that the solubility of the active ingredient in the particle is much larger than in the surrounding fluid, so that in equilibrium the concentration in the particle C_p is related to that in the fluid C_f by $C_p = K_p C_f$ where K_p is the partition coefficient. In general, the volume of the particles V_p will be small compared to the volume of the fluid V_f so the ratio $w = V_p/V_f$ will be small. If the system with initial concentrations C_{p0} in the particles and 0 in the fluid is left until equilibrium is reached with concentrations $C_{p\infty}$ in the particles and $C_{f\infty}$ in the fluid, then the released fraction will be $1/(K_p w + 1)$. In an experiment though, fluid is sampled and replaced hence the active ingredient concentration in the fluid C_f is repeatedly reduced, and more material diffuses out of the particle to re-establish the partition equilibrium. It is therefore possible to approach arbitrarily close to complete release, but on a timescale that is determined by the sampling rate. A similar situation holds in a core-shell particle. If spherical symmetry is assumed, with a core of radius *a*, outer radius of particle *b*, and partition coefficients K_1 between the core and the shell, K_2 between the external fluid and the shell, then if the outer fluid is not replaced during the experiment the final released fraction will be:

$$K_1 / \left(K_1 + K_2 w \sigma^3 + K_1 K_2 w \left(1 - \sigma^3 \right) \right)$$

where $\sigma = a/b$.

In drug release from uniformly dispersed microparticles, where periodic sampling disrupts the established equilibrium by removal of drug from the immediate surrounding of the particles, the frequency of sampling i.e. the rate of drug removal (upsetting the equilibrium) is as important as the solubility of drug in determining how soon complete release of drug occurs. This assumption is confirmed by plots of cumulative drug release versus time (shown in Figures 7a and b) where nearly as much drug was released in a 12-hour study with much frequent sampling (hourly) as in a 7-day study with less sampling frequency. This observation led to further investigation of the influence of sampling frequency on drug release from microparticles.

Figure 7: a) Cumulative release of metformine and glibenclamide from microparticles containing both drugs over 7 days and b) cumulative release of metformine and glibenclamide from microparticles containing both drugs over initial 12-hour period.

The two theoretical models used to explain the impact of sampling frequency on drug release from microparticles, one an analytical model and the other a numerical (finite difference) model, are given as supplementary information.

3.5.3 Release Rate with Sampling

To exemplify the observations, we show in Figure 8a the release rate based on the finite difference results at a set of sampling times, specifically τ= (0.01, 0.02, 0.03, 0.04, 0.05, 0.1, 0.2, 0.4, 0.6, 0.8, 0.9, 1.1, 1.3, 1.5, 1.7, 1.9, 2.1, 2.3, 2.5). These are selected to form a

sequence which is a scaled form of the sampling intervals used in the experiments reported in Section 3.5.1. The control parameter was $K_p w = 10$, and the fraction of fluid withdrawn for sampling at each point was f=0.1. The yellow vertical lines on the graph show the sampling times. One notable feature is that when one shorter sampling interval is introduced (between τ=0.8 and τ=0.9) there is a visible kink in the release graph: this is also observable in the experimental results in Figures 6 and 7.

Figure 8: a) Finite difference predictions of the release fraction obtained with sampling for the case $K_p w$ =10 and sample fraction f=0.1. The yellow vertical lines show the sampling times, b) finite difference predictions of the release fraction obtained with sampling for the case $K_2 w$=10 and sample fraction f=0.1. The blue line shows the evolution of the release, following every step $\Delta\tau$ of the calculation. The red line shows the release profile that would be obtained with constant sampling at a rate f =1, according to equation 32 (in Supplementary Information), and the orange line shows what would be seen without sampling and c) finite difference predictions of the release fraction obtained with different sampling for the case $K_p w$ = 10 and sample fraction f=0.1

Rather more insight can be gained by plotting the release at every time-step, rather than just at the sampling times. This is done in the blue line in Figure 8b, where the release expected predicted for sampling at a steady rate, (equation 32 in Supplementary Information), is shown in red and the result without sampling, (equation 28 in Supplementary Information), is shown in orange. Two points are immediately obvious. First, sampling has had a marked effect on the total release (Figure 8b). Second, within each sample period it is clear that the reduction in solution concentration upsets the local equilibrium at the particle/solution interface, prompting a rapid release to redress the equilibrium, followed by slower release at the rate expected for the current concentration. If uniformly-spaced samples are taken, the resulting release profiles will be smooth, but the results will depend on the sampling interval. This is shown in Figure 8c, where the release fractions are shown for the case $K_2 w = 1$, f=0.1, but with

sampling intervals Δτ=0.10 and Δτ=0.25. We should note that if the sampling interval is decreased so as to follow the earlier part of the release this will itself affect the release rate. An important conclusion is that, because the sampling interval can affect the shape of the release curve, conventional approaches to characterising release mechanisms [24] cannot be applied under these conditions.

4 Clinical Perspectives

In terms of the clinical context of this work, it has the potential to provide a novel and much needed solution to many clinical conundrums. Namely; patient drug compliance, high dosage associated side-affects, poor oral absorption, erratic glycaemic control and therefore a reduction in the morbidity and mortality of diabetes - a common condition that has a rising incidence.

Diabetes is a global pandemic affecting 422 million worldwide - quadruple the number since 1980. The cost of diabetes to the NHS is over £1.5m an hour, this equates to over £25,000 being spent on diabetes every minute and an annual estimated spend of £14 billion, with the cost of treating complications representing a much higher cost. It has micro and macrovascular complications that can have a devastating impact on patient quality of life, ranging from impotence to fulminant renal failure requiring dialysis, blindness and limb amputation in the extreme. The key to its successful treatment is therefore aggressive and tight control of blood sugar and prevention of ongoing hyperglycaemia in the tissues. The combined use of metformin and glibenclamide as in this study provides a multifaceted approach to this, by not only mediating insulin release but also boosting tissue sensitivity to insulin at the same time.

Poor compliance to medication is a huge barrier to effective treatment of diabetes and has long been researched and acknowledged. This problem is complex and thought to be

caused by patient perceived treatment efficacy, medication beliefs, cost of treatment, treatment complexity and convenience, as well as hypoglycaemia and other unwanted side effects such as diarrhoea. Diabetes can often be asymptomatic in the initial stages also affecting attitudes to treatment and medication use. This study could help to combat many of these aspects by reducing the number of drugs and the number of doses needed per day, as well as minimising the side effect profiles. This research also tackles the problem of bioavailability. For example, metformin has an absolute oral bioavailability of 40 to 60%, the drug loaded microparticles designed in this paper would significantly elevate this percentage and boost drug delivery. The promise of future combined drug treatments in the depot microparticle form as routine and mass market prescription for diabetes is an exciting one and further research is needed to facilitate this vision.

5 Conclusions

In this study, we successfully formed, using electrohydrodynamics, a core/shell microparticle systems where active drugs, metformin or glibenclamide or a co-formulation of both drugs, occupied the core of the microparticles while the shell was entirely made of the polymer polymethylsilsesquioxane. While the individual particle sizes was influenced more by the electrical conductivity of the inner solution i.e. the portion forming the core of the particles, particle sphericity and size uniformity within a batch were to a large extent dependent on the flow rate. Therefore, during the formation, flow rates were fine-tuned for the best possible shape of particles and uniformly distributed particles. In terms of molecular composition, FTIR confirmed groups seen in starting materials to be present particles, thus establishing that products indeed contained active drugs as was intended during formation. Furthermore, an XRD scan

between 5^0 and 45^0 (2θ degrees) confirmed the drugs encapsulated within the microparticles existed predominantly in the amorphous state.

At the initial phase of drug release, it was observed that a higher amount of the more soluble metformin was released compared to the less soluble glibenclamide. This was expected and largely attributed to the higher water solubility of metformin driving up diffusion from the microparticle into the dissolution media. Significant initial bursts seen in all particles were analysed and were most likely caused by drug diffusing through the shell onto the particle surface through solvent evaporation during particle formation.

A mathematical model of the system has been developed, based on the key parameters at play such as the core/shell structure, extent of partitioning of drugs between these two layers, dissolution volume and its rate of refreshment. This has allowed a more detailed understanding of how drugs could be released from a two-layered system. The frequency of sampling is shown to upset the equilibrium at the interface between the particle and the release medium; the additional release required to reset this equilibrium has been shown to significantly influence the overall amount of drug released.

Data accessibility

All relevant data are presented in the main text. Further information, particularly on the mathematical analyses are presented in the electronic supplementary material. We will provide these data, upon request, in an electronic format.

Authors' contributions

TS and FB designed the study and the experiments, performed experiments, analysed the data and drafted the initial version of manuscript. SH conducted the focused ion beam (FIB) imaging on particles analysed in this study. AHH conducted the mathematical modelling on experimental data and helped with interpreting release data. UE offered clinical perspectives on this work and elaborated on the prospects of alternate antidiabetic formulations. ME advised on the design of experiments as well as revising the initial draft of the manuscript. All authors gave final approval for publication and agree to be held accountable for the work performed therein.

Competing interests

We declare we have no competing interests.

References

[1] Yoshida, Y. & Simoes, E.J. 2018 Sugar-Sweetened Beverage, Obesity, and Type 2 Diabetes in Children and Adolescents: Policies, Taxation, and Programs. *Curr. Diabetes Rep* . **18**, 1-10.

[2] Zheng, Y., Ley, S.H. & Hu, F.B. 2017 Global Aetiology and Epidemiology of Type 2 Diabetes Mellitus and Its Complications. *Nat. Rev. Endocrinol.* **14**, 88-98

[3] Chaudhury, A., Duvoor, C., Dendi, R., Sena, V., Kraleti, S., Chada, A., Ravilla, R., Marco, A., Shekhawat, N.S. & Montales, M.T. 2017 Clinical Review of Antidiabetic Drugs: Implications for Type 2 Diabetes Mellitus Management. *Front. Endocrinol* **8**, 1-12.

[4] Cheng, A.Y. & Fantus, I.G. 2005 Oral Antihyperglycemic Therapy for Type 2 Diabetes Mellitus. *Can. Med. Assoc. J.* **172**, 213-226.

[5] DeFronzo, R. 1992 Pathogenesis of Type 2 (Non-Insulin Dependent) Diabetes Mellitus: A Balanced Overview. *Diabetologia* **35**, 389-397.

[6] Tosi, F., Muggeo, M., Brun, E., Spiazzi, G., Perobelli, L., Zanolin, E., Gori, M., Coppini, A. & Moghetti, P. 2003 Combination Treatment with Metformin and Glibenclamide Versus Single-Drug Therapies in Type 2 Diabetes Mellitus: A Randomized, Double-Blind, Comparative Study. *Metabolism* **52**, 862-867.

[7] Aittoniemi, J., Fotinou, C., Craig, T.J., de Wet, H., Proks, P. & Ashcroft, F.M. 2009 Sur1: A Unique Atp-Binding Cassette Protein That Functions as an Ion Channel Regulator. *Philos. Trans. R. Soc., B* **364**, 257-267.

[8] Rena, G., Hardie, D.G. & Pearson, E.R. 2017 The Mechanisms of Action of Metformin. *Diabetologia* **60**, 1577-1585.

[9] Cramer, J.A. 2004 A Systematic Review of Adherence with Medications for Diabetes. *Diabetes care* **27**, 1218-1224.

[10] Desai, D., Wang, J., Wen, H., Li, X. & Timmins, P. 2013 Formulation Design, Challenges, and Development Considerations for Fixed Dose Combination (FDC) of Oral Solid Dosage Forms. *Pharm. Dev. Technol.* **18**, 1265-1276.

[11] Kohane, D.S. 2007 Microparticles and Nanoparticles for Drug Delivery. *Biotechnol. Bioeng.* **96**, 203-209.

[12] Bock, N., Dargaville, T.R. & Woodruff, M.A. 2012 Electrospraying of Polymers with Therapeutic Molecules: State of the Art. *Prog. Polym. Sci.* **37**, 1510-1551.

[13] Orlu-Gul, M., Topcu, A.A., Shams, T., Mahalingam, S. & Edirisinghe, M. 2014 Novel Encapsulation Systems and Processes for Overcoming the Challenges of Polypharmacy. *Curr. Opin. Pharmacol.* **18**, 28-34.

[14] Mehta, P., Haj-Ahmad, R., Rasekh, M., Arshad, M.S., Smith, A., van der Merwe, S.M., Li, X., Chang, M.-W. & Ahmad, Z. 2017 Pharmaceutical and Biomaterial Engineering Via Electrohydrodynamic Atomization Technologies. *Drug Discovery Today* **22**, 157-165.

[15] Nangrejo, M., Ahmad, Z., Stride, E., Edirisinghe, M. & Colombo, P. 2008 Preparation of Polymeric and Ceramic Porous Capsules by a Novel Electrohydrodynamic Process. *Pharm. Dev. Technol.* **13**, 425-432.

[16] Chang, M.-W., Stride, E. & Edirisinghe, M. 2010 Controlling the Thickness of Hollow Polymeric Microspheres Prepared by Electrohydrodynamic Atomization. *J. R. Soc., Interface* **7**, S451-S460.

[17] Cetin, M. & Sahin, S. 2016 Microparticulate and Nanoparticulate Drug Delivery Systems for Metformin Hydrochloride. *Drug delivery* **23**, 2796-2805.

[18] Singh, A., Worku, Z.A. & Van den Mooter, G. 2011 Oral Formulation Strategies to Improve Solubility of Poorly Water-Soluble Drugs. *Expert Opin. Drug Delivery* **8**, 1361-1378.

[19] Savjani, K.T., Gajjar, A.K. & Savjani, J.K. 2012 Drug Solubility: Importance and Enhancement Techniques. *ISRN Pharm.* **2012**, 1-11

[20] Elbahwy, I.A., Ibrahim, H.M., Ismael, H.R. & Kasem, A.A. 2017 Enhancing Bioavailability and Controlling the Release of Glibenclamide from Optimized Solid Lipid Nanoparticles. *J. Drug Delivery Sci. Technol* **38**, 78-89.

[21] Essa, E.A., Elkotb, F.E., Eldin, E.E.Z. & El Maghraby, G.M. 2015 Development and Evaluation of Glibenclamide Floating Tablet with Optimum Release. *J. Drug Delivery Sci. Technol* **27**, 28-36.

[22] Shams, T., Parhizkar, M., Illangakoon, U., Orlu, M. & Edirisinghe, M. 2017 Core/Shell Microencapsulation of Indomethacin/Paracetamol by Co-Axial Electrohydrodynamic Atomization. *Mater. Des.* **136**, 204-213.

[23] Gibaldi, M. & Feldman, S. 1967 Establishment of Sink Conditions in Dissolution Rate Determinations. Theoretical Considerations and Application to Nondisintegrating Dosage Forms. *J. Pharm. Sci.* **56**, 1238-1242.

[24] Ritger, PL, Peppas, NA. 1987 A simple equation for description of solute release I. Fickian and non-Fickian release from non-swellable devices in the form of slabs, spheres, cylinders or discs. *J. Controlled Release* **5**, 23-36.
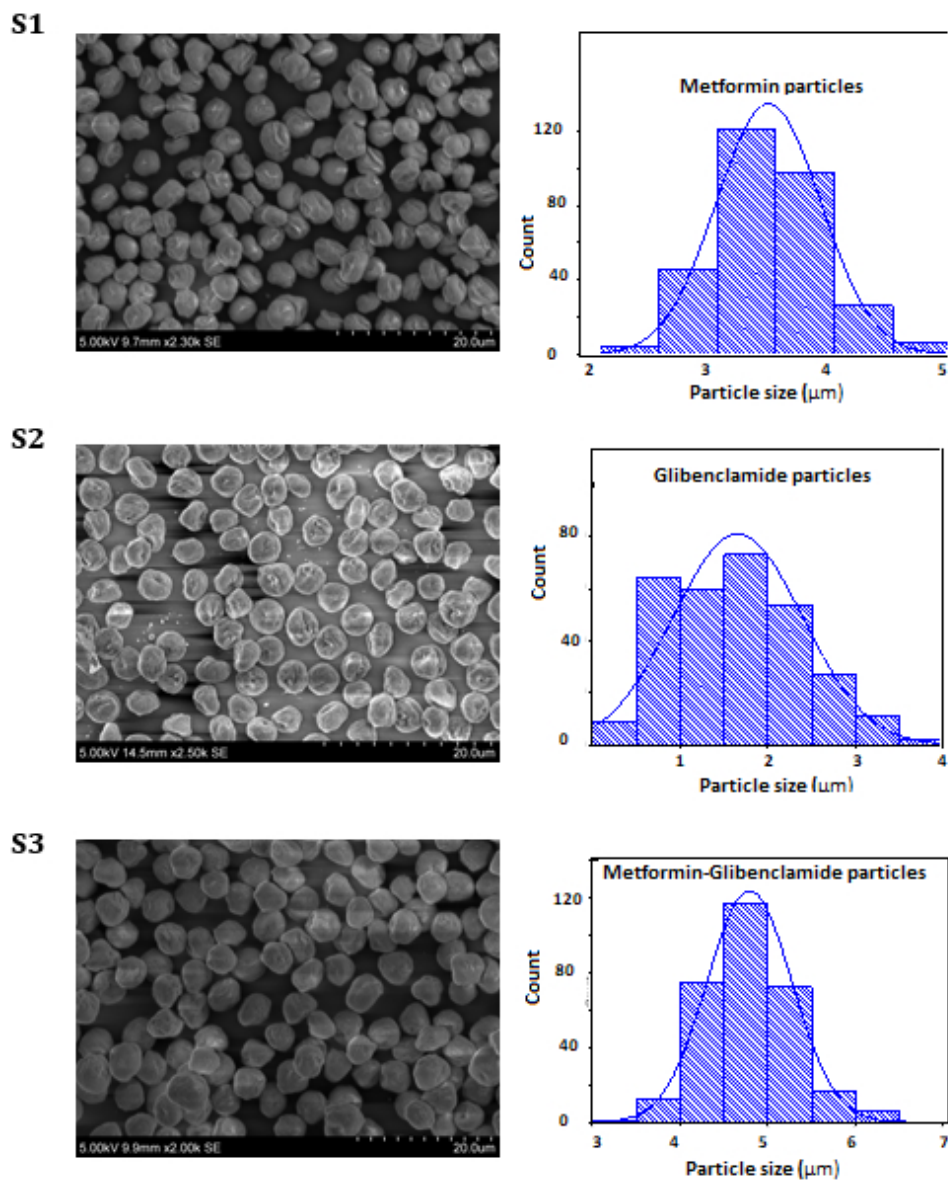
Figure 1: SEM images and the corresponding size distribution graphs of the developed drug delivery systems S1, S2 and S3. The smooth curve superimposed on each histogram represents a normal distribution with the same mean and standard deviation as the sample.
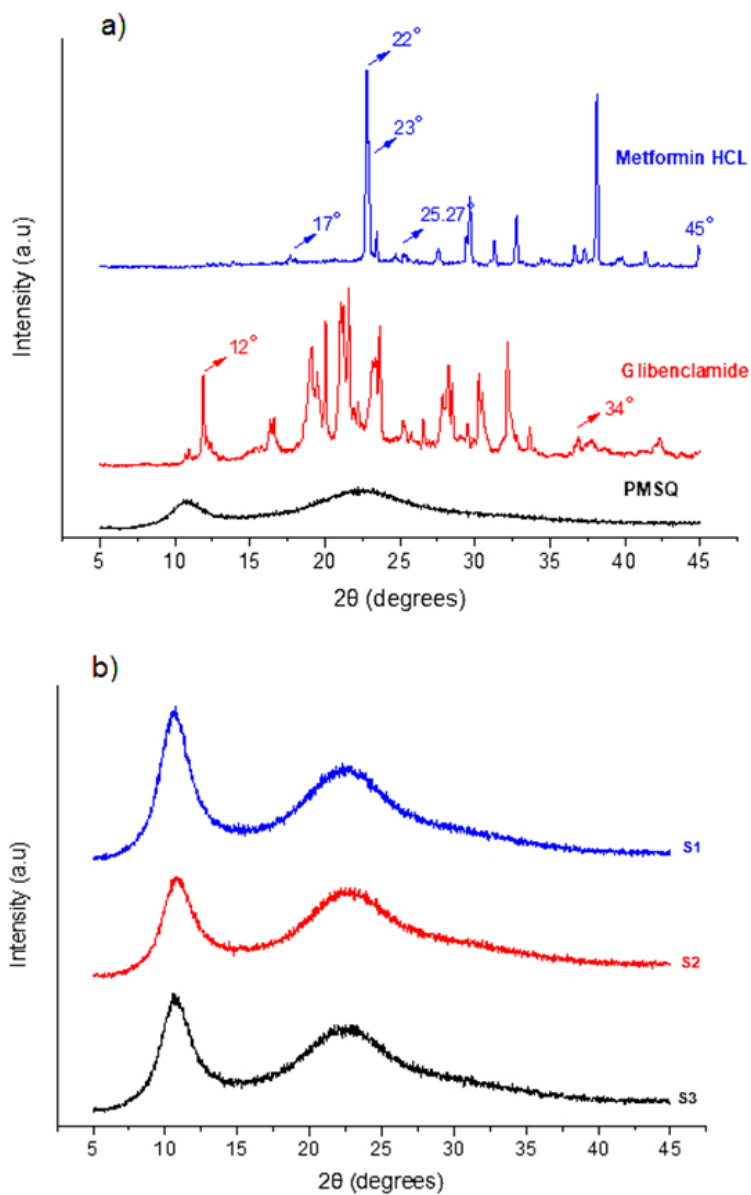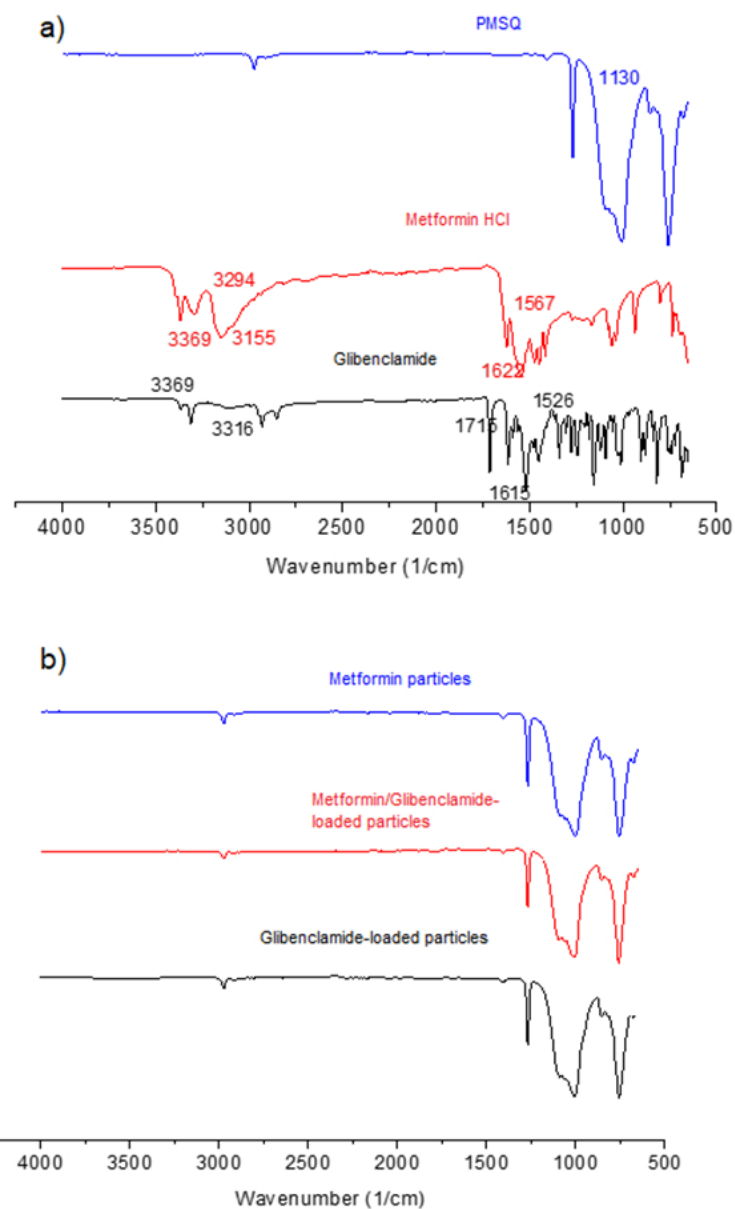
133x160mm (96 x 96 DPI)

Figure 2 XRD spectrum of a) pure metformin HCL, glibenclamide and PMSQ and b) the developed formulations S1, S2 and S3.

151x229mm (96 x 96 DPI)

Figure 3 FTIR spectra of pure PMSQ, metformin HCL, glibenclamide and the developed formulations S1, S2 and S3.
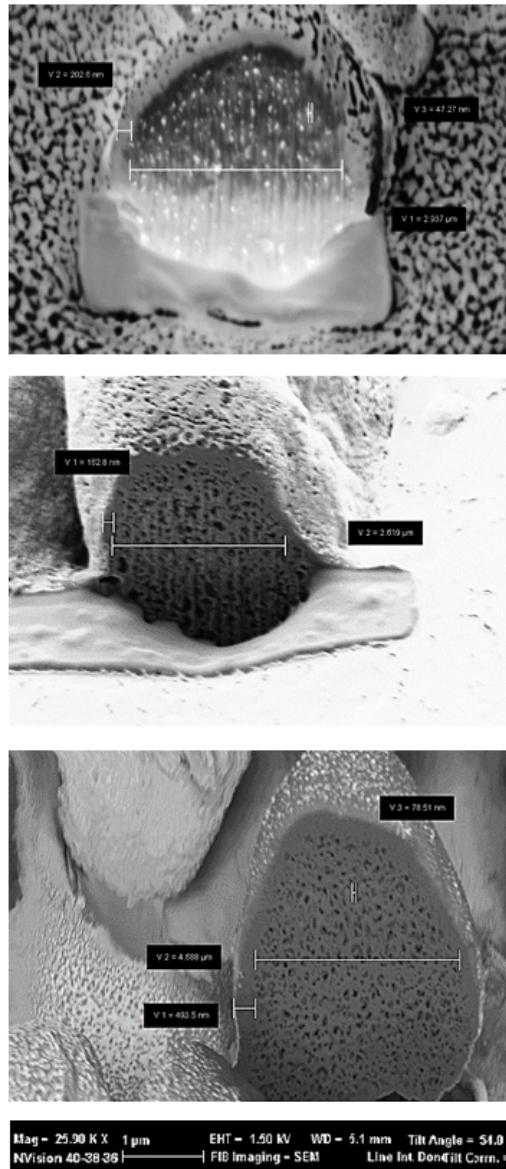
151x238mm (96 x 96 DPI)

Figure 4 Fig. 5. SEM/FIB cross-section images of the prepared formulations S1, S2 and S3.
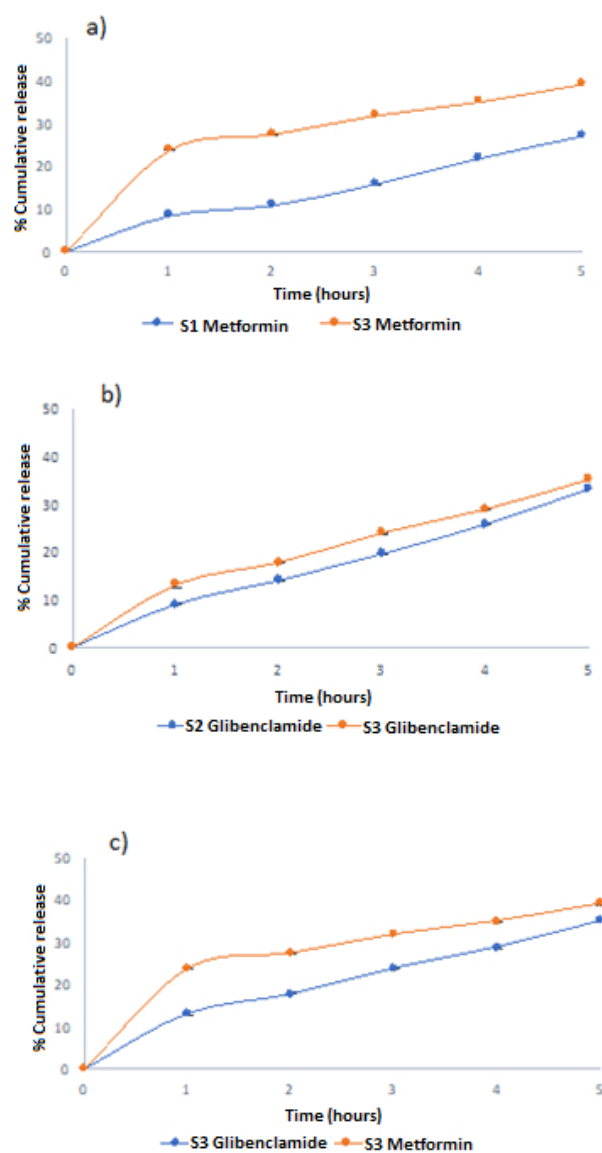
96x220mm (96 x 96 DPI)

Figure 5: Cumulative drug release in the first 5 hours of a) metformin from S1 and S3 formulations b) glibenclamide from S2 and S3 formulations and c) cumulative release of glibenclamide and metformin percentage cumulative release from S3.
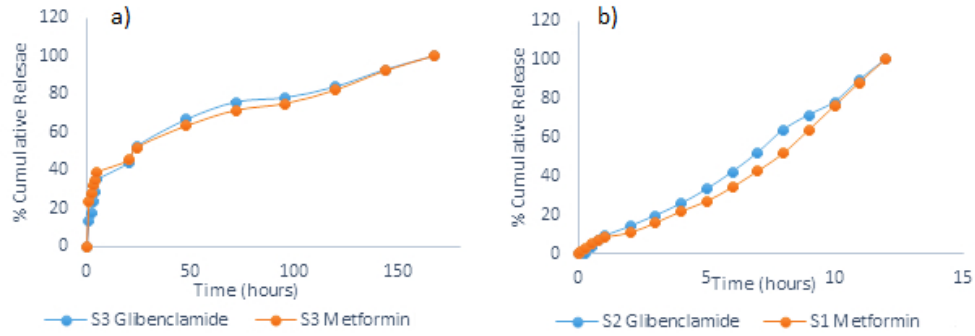
96x187mm (96 x 96 DPI)

Figure 6 a) Glibenclamide and metformin cumulative release from S3 and b) glibenclamide and metformin cumulative release from S2 and S1.
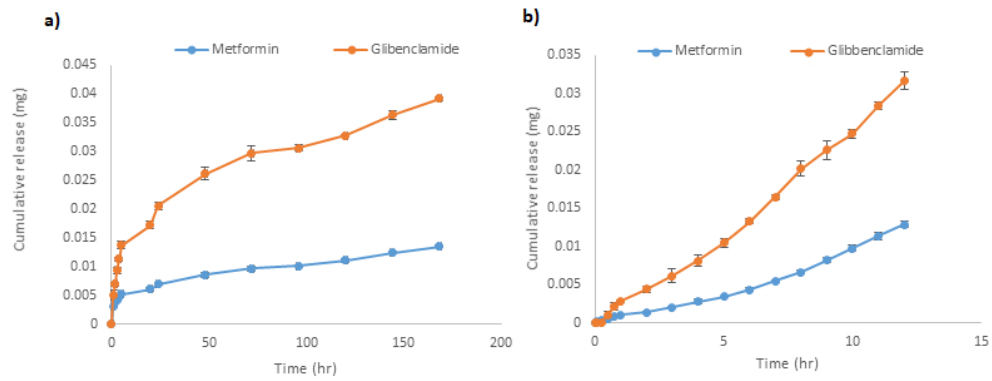
162x69mm (96 x 96 DPI)

Figure 7: a) Cumulative release of metformine and glibenclamide from microparticles containing both drugs over 7 days and b) cumulative release of metformine and glibenclamide from microparticles containing both drugs over initial 12-hour period.
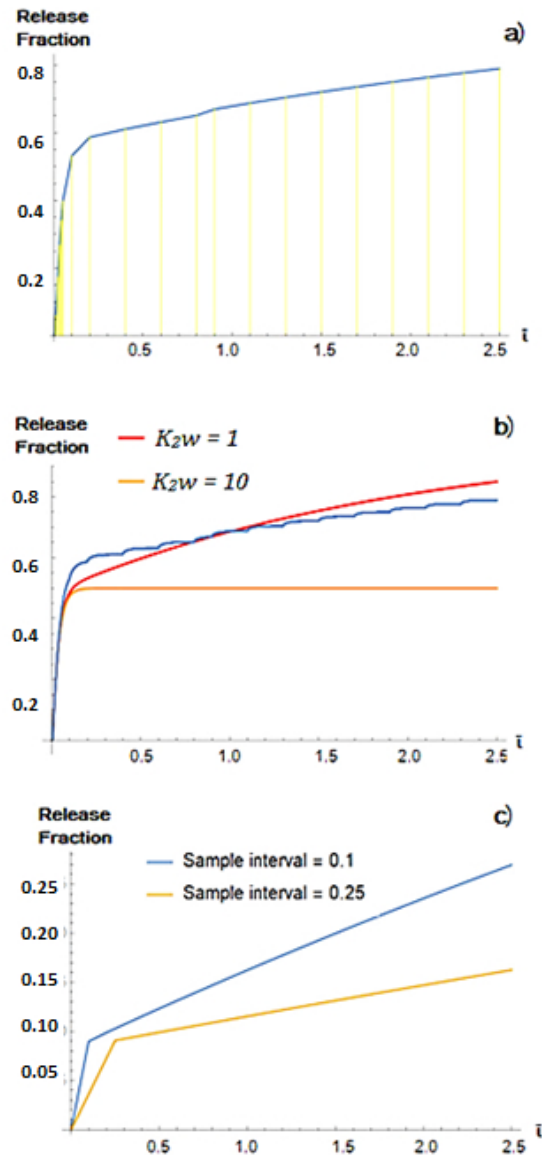
211x85mm (96 x 96 DPI)

1
2
3
4
5
6
7
8
9
10
11
12
13
14
15
16
17
18
19
20
21
22
23
24
25
26
27
28
29
30
31
32
33
34
35
36
37
38
39
40
41
42
43
44
45
46
47
48
49
50
51
52
53
54
55
56
57
58
59
60

Figure 8: a) Finite difference predictions of the release fraction obtained with sampling for the case Kpw =10 and sample fraction f=0.1. The yellow vertical lines show the sampling times, b) finite difference predictions of the release fraction obtained with sampling for the case K2w=10 and sample fraction f=0.1. The blue line shows the evolution of the release, following every step Δτ of the calculation. The red line shows the release profile that would be obtained with constant sampling at a rate f =1, according to equation 32 (in Supplementary Information), and the orange line shows what would be seen without sampling and c) finite difference predictions of the release fraction obtained with different sampling for the case Kpw = 10 and sample fraction f=0.1

87x179mm (96 x 96 DPI)